Application of a Hybrid Controller with Non-Contact Impedance to a Humanoid Robot

Baris Ulutas, *Member IEEE*, Erdem Erdemir, *Member IEEE*, Kazuhiko Kawamura, *Fellow IEEE*
Center for Intelligent Systems
Vanderbilt University
37235-0131 Nashville, TN, USA
Emails: (baris.ulutas, erdem.erdemir, kazuhiko.kawamura) @vanderbilt.edu

Abstract— **This paper addresses the design issues of a hybrid neural network-based PID control with grey prediction and non-contact impedance as applied to a humanoid robot named ISAC. ISAC uses two six degree-of freedom manipulators called Soft Arms which are actuated by pneumatic artificial muscles. High nonlinearities such as hysteresis and unknown dynamics of these muscles make arm control a challenging task. ISAC was designed to assist physically challenged, thehefore it has to fulfill safety precautions concerning its movements. To evaluate the proposed controller, it was tested for human-like grasping motions while guaranteeing the safe interaction with humans. The controller consists of two sub-controllers, an open-loop neural network-based controller which is managed by non-contact impedance and powered by grey prediction.**

I. Introduction

A. Related Literature

Extensive experimental studies have been carried out to identify biological control strategies of human arms and hands. Humans can perform a variety of dexterous movements by adjusting dynamic characteristics of the musculoskeletal system in motion. For example, a volleyball player can serve an extraordinarily fast ball through controlling his arm dynamics and creating an arc-shaped movement of his arm. The momentum of the ball depends not only on the strong muscle power of the player, but also on the ability to freely control his arm dynamics and learned skills. Much research has been done on human movements and often described with mechanical impedance parameters; stiffness, viscosity, and inertia [1][2]. Gomi et al. [3] and Tsuji et al. [4] included arm movement and examined human hand characteristics, including inertia, viscosity and stiffness in multi-joint arm movements.

Artificial pneumatic muscles [5][6] are often adopted by designers for several reasons because they provide safe human-robot interaction and have high power/weight ratios. Although these muscles are superior in some respects to standard robotic arms using electrical motors, controlling these muscles is extremely difficult due to nonlinear characteristics. This high nonlinearity stems from poor damping ability, delays from valve operations and the changes in parameters during usage [7][8][9][10]. In order to deal with these problems, various close-loop feedback controllers have been proposed. They range from basic PID [11] and fuzzy+PID [12] controllers to more sophisticated neural network [13] and sliding mode [7] controllers. Since response is extremely slow and actuators are compliant in nature, pneumatic muscle-based systems the feedback loop can result in instability. Sliding mode control can solve these types of problems but one disadvantage is chattering which results in instability. Chattering increases the load of the controller, damages the artificial pneumatic muscles and shortens the life-time of the artificial pneumatic muscles.

Artificial neural networks (ANNs) offer good performance to deal with inputs having various ranges [14], to create mappings between the reference signals and the arm movements, and to be used as an open-loop controller to reduce the problems associated with artificial muscle-based systems. The change in the parameters of the artificial muscles requires repeated training of ANNs. However, in our controller we use ANNs to bring the end-effector to the vicinity of the goal position. By not requiring an exact positioning, ANNs do not need further training. After reaching the vicinity of the goal position, a PID controller with non-contact impedance and grey prediction takes action to bring end-effector to the goal.

Impedance control is generally used as a way to control the mechanical impedance of an end-effector in an environment where interaction forces are important. An innovative work by Hogan [15] introduced a method to control end-effector impedance. Other researchers followed Hogan's work [16][17][18]. The interaction forces are controlled after a contact occurs and relied on force sensors for their feedbacks.

In grasping, it is better to control the end-effector before any contacts with the target object occur. In this way, the task of grasping of any fragile object that requires a careful grasp is better handled. Castano proposed the concept "visual compliance", a basis for non-contact impedance control [19][20].

Deng introduced the grey system theory in [21]. As a predictor for systems with partially unknown parameters or no exact system dynamic model, the grey theory has been proven to enable to increase the performance of classical controllers [23][24]. The integration of a grey predictive control into PID control with impedance does not only simplify the design procedure but also improves the controller performance.

In our research, we used a controller consisting of two sub-controllers. ANNs are used for reaching the vicinity of the end-effector. At a point where end-effector gets closer to the goal, PID control with non-contact impedance takes over for

978-1-4244-2200-5/08/$25.00 ©2008 IEEE

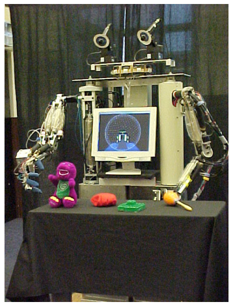

Fig. 1. ISAC- Intelligent Soft Arm Control Robot

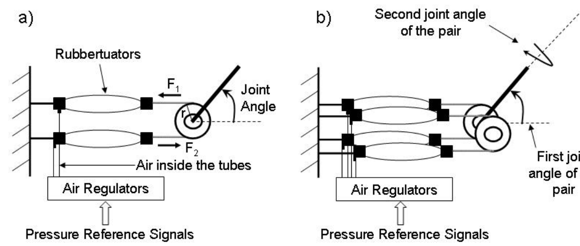

Fig. 2. a) A pair of artificial pneumatic muscles can produce a revolute joint about the axis of the pulley connecting the two ends of the artificial pneumatic muscles. b) Two pairs of artificial pneumatic muscles can produce two revolute joints about the axis of the pulley connecting the ends of the artificial pneumatic muscles.

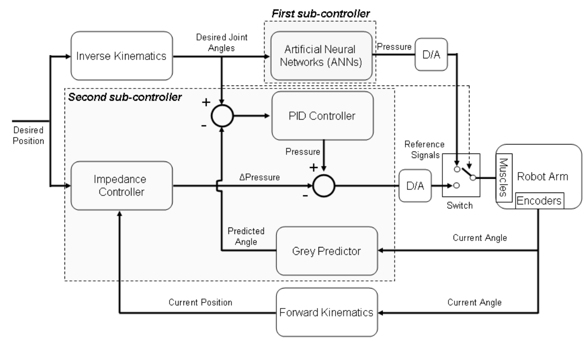

Fig. 3. Controller structure

bringing the end-effector to the goal position. Grey predictor is utilized for PID controller with non-contact impedance to overcome delay problems associated with the artificial pneumatic muscles.

B. Overview

This paper is divided into six sections. In section 1, brief information about the subject and related literature was presented. Section 2 examines the system to be used for experimentation. In section 3, the proposed controller structure is defined and mathematical equations are given. In Section 4, experimental results of the theory developed are presented with comparisons to PID control without grey prediction and non-contact impedance. The last two sections present the experimental results and the planned future work.

II. Experimental Platform

ISAC (see Fig. 1) is an upper-torso humanoid robot with two 6-degree-of-freedom arms that are actuated pneumatically by artificial pneumatic muscles which provide a relatively safe human-robot interaction for manipulation, automation and other tasks. ISAC kinematics are very close to the PUMA 560 kinematics, which is solved in [25].

Because the artificial pneumatic muscles are unidirectional actuators, two antagonistic coupled artificial pneumatic muscles are needed to actuate a revolute joint as shown in Fig. 2. Whereas both position and compliance of the joints are determined by the artificial pneumatic muscle pressures, controlling the antagonistic joint actuator is therefore done by controlling the pressures. These pressures are controlled by electro-pneumatic regulators. These regulators have very fast acting valves (sampling time = 4ms) that set the pressure at a level proportional to the valve signal input voltage.

The first two joints of the arms are actuated by antagonistic and agonist artificial pneumatic muscle pair. The third and the forth joints are differential pairs, this means that four artificial pneumatic muscles (two pairs of are antagonistic and agonist artificial pneumatic muscles) are linked together to control two revolute joints, intersect at a point as shown Fig. 2b. This system was inspired from human elbow and wrist structure. For example, a person can turn his hands to face down or up and at the same time, we can move our hands up and down, by the contradiction and relaxation of forearm muscles. The last two joints are also differential pairs.

ISAC is also equipped with an active stereo vision system. Using two cameras which pan and tilt independently. This system is used to localize objects in ISAC workspace.

III. Controller

Our controller consists of two sub-controllers. For the first sub-controller, we use a simple mapping between joint angles to input voltages of the valves by using ANNs. The second is a PID controller with additional impedance. The controller structure is shown in Fig. 3.

A virtual sphere with radius r, which equals to pre-specified distance, is located at the goal position as in [20]. If the end-effector's distance to goal is bigger than the pre-specified distance, the controller uses ANNs which map the joint angles to input voltages of valves. Although ANNs have various advantages over other type of controllers in this particular case, it cannot guarantee the reaching of the goal state. In order to guarantee reaching and grasping, the controller switches to the PID controller with impedance after the end-effector gets closer to the goal position than the pre-specified distance. Additionally a grey predictor is utilized for improving the performance of the PID controller.

A. ANN Controller

The soft computing method used as a controller here is the well-understood back-propagation neural network with the generalized delta rule employed as the learning mechanism.

The main motivation of using ANNs in our controller is its capability of learning the relation between the air regulator input references and the joint motion, which is nonlinear and involves hysteresis. The frictional forces between the rubber tube and the sleeve cause this hysteresis problem. To overcome control problems associated with the hysteresis, two different ANNs are trained for opposite motion directions of the same joint.

The ANNs used to map joint angles to the input voltages of valves have a simple structure with an input layer, a hidden layer and an output layer. While input layer and output layers consist of one neuron each, ten neurons were used for the hidden layer. Sigmoid function is used as the activation function and the nets are trained in ten thousand epochs with approximately two hundred samples.

B. PID Controller with Impedance

The main motivation in the selection of the PID controller with impedance is its applicability of our planned future work titled "learning grasping affordances". In this future work, learning is claimed to be achieved by adaptively changing the impedance parameters. Moreover, impedance part of the controller allows us to control the position and the velocity of the end-effector directly, which is crucial for dexterous grasping.

To realize the switching between ANNs and the PID controller with virtual impedance, a sphere of predetermined radius is assumed to be located at the goal position as in [20]. When the end-effector penetrates through the boundary of this sphere, the PID controller with impedance takeovers the control from ANNs for dexterous grasping.

Furthermore, in this work the PID controller's performance is improved by grey prediction, which is used to reduce delays by prediction of the future output values of the joint angles. As will be shown by experiments, the grey predictors work well in reducing the overshoots which are almost inevitable in systems where controller switching takes place.

1) Mathematical Foundation of the PID Controller with Impedance: The dynamic equation for an n-joint manipulator can be represented in a general state-space form as follows:

$$M(\Theta)\ddot{\Theta} + V(\Theta, \dot{\Theta}) + G(\Theta) = \tau, \tag{1}$$

where Θ is the $nx1$ joint angle vector, $M(\Theta)$ is the nxn mass matrix of the manipulator, $V(\Theta, \dot{\Theta})$ is an $nx1$ vector of centrifugal and Coriolis terms, $G(\Theta)$ is an $nx1$ vector of gravity terms, and τ is the $nx1$ joint torque vector.

In order to control the manipulator, a τ vector needs to be designed and supplied to joints. Since in our case $M(\Theta), V(\Theta, \dot{\Theta}), G(\Theta)$ are all unknown, a model-based controller cannot be designed for controlling the end-effector position. Considering this fact and the reasons mentioned in the previous sections, we focus our attention on two control schemes -ANNs and PID- for controlling the soft arm. A virtual impedance is placed between the end-effector and goal position for dexterous grasping. In the proposed controller, at the outside of the virtual sphere, τ is supplied by the ANNs.

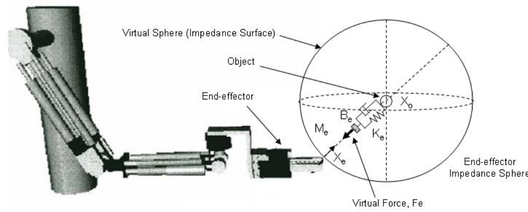

Fig. 4. Virtual sphere and impedance

After entering the virtual sphere, the controller switches to the PID controller with impedance, where τ can be expressed in the following form:

$$\tau = \tau_{PID} + \tau_e, \tag{2}$$

where $\tau_{PID} \in \mathbf{R^n}$ is the torque supplied by the PID controller and $\tau_e \in \mathbf{R^n}$ is the torque resulted from the impedance designed for an dexterous grasp.

The virtual impedance added to the end-effector slows down motion when the end-effector approaches to its goal position. Fig. 4 shows both the virtual sphere and the associated virtual impedance added to the end-effector. Mathematical notations follow the notations in [20]. When the end-effector enters the virtual sphere, the displacement vector $X_r \in \mathbf{R^3}$ is given by the following equation:

$$X_r = X_e - X_o, \tag{3}$$

where $X_e \in \mathbf{R^3}$ is the position of the end-effector and $X_o \in \mathbf{R^3}$ is the center of the virtual sphere where object is located. The corresponding normal vector from surface of the sphere to the end-effector position can be defined by the following equation:

$$dX_e = X_r - ra \tag{4}$$

where $r \in \mathbf{R}$ is the radius of the virtual sphere and $a \in \mathbf{R^3}$ is defined as:

$$a = \begin{cases} \frac{X_r}{|X_r|} & (|X_r| \neq 0) \\ 0 & (|X_r| = 0) \end{cases}, \tag{5}$$

where $|X_r| \in \mathbf{R}$ is the norm of X_r.

The force associated with the virtual impedance can be calculated from the following equation:

$$F_e = \begin{cases} M_e d\ddot{X}_e + B_e d\dot{X}_e + K_e dX_e & (|X_r| < r) \\ 0, & (|X_r| > r) \end{cases}, \tag{6}$$

where $M_e, B_e, K_e \in \mathbf{R^{3x3}}$ are the virtual inertia, the viscosity and the stiffness matrices.

The virtual force calculated as above can be distributed to the individual joints by:

$$\tau_e = J^T(\Theta) F_e, \tag{7}$$

where $J(\Theta) \in R^{3xn}$ Jacobian matrix associated with the goal position. The Jacobian matrix of the soft arm is calculated by measuring various link lengths. Since there could be errors in the measurements, the distribution of the force to joints might not be the exact one. However, grey prediction used also compensates the errors associated with the Jacobian.

In the soft arm, the torque is supplied to joints by creating a pressure difference between two artificial pneumatic muscles that are antagonist (See Fig. 2). The relationship between the pressure difference $\Delta P \in \mathbf{R}$ and the torque $\tau_m \in \mathbf{R}$ is defined in [22] by:

$$\Delta P = \frac{\tau_m}{2h(\beta - \alpha\epsilon)} - \frac{\gamma}{(\beta - \alpha\epsilon)}, \tag{8}$$

where h is the radius of the pulley system that connects the antagonist pneumatic muscles, β, γ and α are artificial pneumatic muscle specific constants and ϵ is defined as:

$$\epsilon = \frac{(L_0 - L)}{L_0}, \tag{9}$$

where L_0 is the initial and L is the present length of an artificial pneumatic muscle.

The relationship between τ_m and ΔP is used to calculate ΔPs associated with the τ_e. For the i^{th} joint the pressure difference ΔP_i can be calculated as follow:

$$\Delta P_i = \frac{\tau_{e_i}}{2h(\beta - \alpha\epsilon)} - \frac{\gamma}{(\beta - \alpha\epsilon)}, \tag{10}$$

where $\tau_{e_i} \in \mathbf{R}$ is the torque distributed to the i^{th} joint.

Then, inside the virtual sphere, the i^{th} joint is controlled as follows:

$$\begin{array}{l} P_{i1}^{t+1} = P_{i1}^{t} + (K_{P_i} e^t + K_{D_i} \dot{e^t} + K_{I_i} \int e^t dt - \Delta P_i^t) \\ P_{i2}^{t+1} = P_{i2}^{t} - (K_{P_i} e^t + K_{D_i} \dot{e^t} + K_{I_i} \int e^t dt - \Delta P_i^t) \end{array}, \tag{11}$$

where $P_{i1}, P_{i2} \in \mathbf{R}$ are the pressures of antagonist muscles of i^{th} joint, $K_{P_i}, K_{D_i}, K_{I_i}$ are the PID parameters, $e = (\theta_i - \theta_d) \in \mathbf{R}$ is the error between current θ_i and desired θ_d joint angles, and ΔP_i is the pressure difference resulted from the distribution of the impedance force. The superscripts t and $t+1$ are used to represent the current and next step values of the variables.

As getting closer to the object the effect of impedance exceeds that of PID controllers. Thus a threshold for individual joints is needed to be defined for reaching the goal position. A threshold for the i^{th} joint $\zeta_i \in \mathbf{R}$ is defined as:

$$\zeta_i = 0.8(K_{P_i} e^t + K_{D_i} \dot{e^t} + K_{I_i} \int e^t dt) \tag{12}$$

If ΔP_i exceeds calculated threshold value, its value is equated to the ζ_i value.

2) Grey Predictor: In order to improve the performance of the PID controller with impedance, we utilize a grey predictor for each individual joint of type GM(1,1) (the first-order one-variable grey differential equation model) which is capable of predicting future output joint angle values. By using the predicted joint angles, the impacts of problems associated with the time delays in muscles are decreased. As a result, which will be shown in the experimental results section, the overshoots are reduced in the system response considerably.

In this model, in order to reduce the randomness of the data, an operator called Accumulating Generation Operation (AGO) is applied. Accumulated data will be used to find the parameters of first-order differential equation of GM11. From differential equation, which is specified by the calculated parameters, future values of the accumulated data are predicted. In order to get the actual predicted values of the system, an operator named Inverse Accumulating Generation Operation (IAGO) is applied to the predicted accumulated data values.

Here is a brief summary of the grey systems theory [23]. Let's assume we have the system output as a non-negative time sequence data as follows:

$$D^{(0)} = (d^{(0)}(1), d^{(0)}(2), d^{(0)}(3), \ldots, d^{(0)}(n)), n \geq 4 \tag{13}$$

where n is the sample size. AGO is applied to this primitive data to smooth the randomness. Obtained new sequence with reduced randomness is as follows:

$$D^{(1)} = (d^{(1)}(1), d^{(1)}(2), d^{(1)}(3), \ldots, d^{(1)}(n)), n \geq 4 \tag{14}$$

where

$$d^{(1)}(k) = \sum_{i=1}^{k} d^{(0)}(i), k = 1, 2, \ldots, n \tag{15}$$

Then, the mean sequence data, $Z^{(1)}$, of $D^{(1)}$ can be found as follows:

$$Z^{(1)} = (z^{(1)}(2), z^{(1)}(3), \ldots, z^{(1)}(n)) \tag{16}$$

where

$$z^{(1)}(k) = \frac{1}{2} d^{(1)}(k) + \frac{1}{2} d^{(1)}(k-1) \tag{17}$$

The least square estimate sequence is defined by the following equation:

$$d^{(0)}(k) + a z^{(1)}(k) = b \tag{18}$$

The corresponding whiting equation is as follows:

$$\frac{d[d^{(1)}(t)]}{dt} + a d^{(1)}(t) = b \tag{19}$$

The parameters a and b can be found by using the following equation:

$$< a, b > = (B^T B)^{-1} B^T \overrightarrow{Y} \tag{20}$$

where

$$\overrightarrow{Y} = < d^{(0)}(2), d^{(0)}(3), \ldots, d^{(0)}(n) > \tag{21}$$

and

$$B = \begin{bmatrix} -z^{(1)}(2) & 1 \\ -z^{(1)}(3) & 1 \\ . & . \\ . & . \\ -z^{(1)}(n) & 1 \end{bmatrix} \tag{22}$$

In Equation 19, the solution for $d^{(1)}(t)$ is as follows:

$$d_p^{(1)}(k+1) = [d^{(0)}(1) - \frac{b}{a}] e^{-ak} + \frac{b}{a} \tag{23}$$

In order to predict the output of the system, IAGO is applied. The predicted value can be obtained as follows:

$$d_p^{(0)}(k+H) = [d^{(0)}(1) - \frac{b}{a}] e^{-(k+H+1)} (1 - e^{a}) \tag{24}$$

where H is the step size of the prediction.

In this work, we used a window size of 5 and a step size 2 for an individual grey predictor. In other words, 5 previous values are used to predict 2 step afterwards of the output joint angle. Instead of feeding current output value, the predicted value was used for the PID controller.

IV. Experimental Results

The applicability of the theory is investigated by experimenting on ISAC's left arm. As mentioned earlier, instead of comparing the results with other controllers which can be applied to unknown dynamics system, we only consider the applicability of the theory. Our planned future work, in which ISAC will learn how to grasp objects, there is a need for a controller that can enable us to adaptively control end-effector position and velocity. This work will constitute a foundation for future work.

The location of the object was determined by using the stereo vision system and a virtual impedance sphere, with a radius of 100 mm, was placed around that object. Performance of the controller is presented in Fig. 5. For comparison purposes, the results obtained from solely application of neural nets and controller without grey prediction are also presented. From given figure, one can easily distinguish the two controllers. As mentioned earlier, while neural networks are used for perfunctory movement to the goal, the neuro-PID controller with grey prediction and impedance takes the control for the final steps for dexterous grasping. The results shown confirm that a goal of smoothly reaching the end position by mimicking humanoid motion has been realized. Fig. 5 illustrates that neural networks can be used for reaching the neighborhood of the goal position from a distant location. After reaching the neighborhood, PID control with impedance slowly settles the end-effector to the final position. However, at the line that separates the two controllers, we see some damped oscillations. These oscillations are the result of perfunctory movements realized by the neural networks and the natural delays associated with the muscles.

In order to reduce the amplitude of the oscillations, grey predictors were added to the individual PID controllers of joints in the system. Fig. 6 shows a zoomed portion of Fig. 5 for a better look. As can be deduced from the figure, the grey predictors are pretty good in improving the performance of the controller. With the help from grey predictors, we can account for delays in the system. Grey predictors also exhibit some filtering ability by reducing the chattering like responses which resulted during switching of the controller. Sliding mode controllers, however, are not suitable for pneumatic muscle type actuators where chattering shortens the life-time of the actuators.

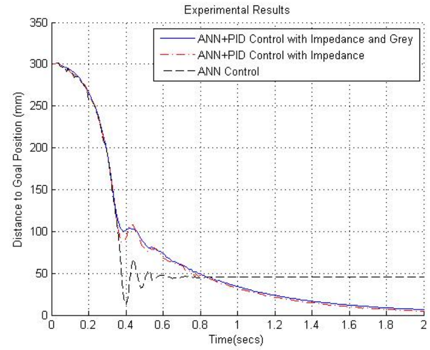

Fig. 5. Experiment Results: Neuro-Impedance with Grey, Neuro-Impedance and Neural Controllers

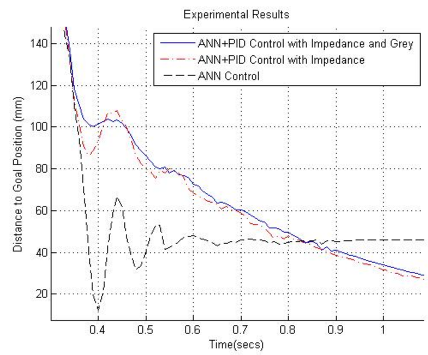

Fig. 6. Zoomed Version of Experiment Results: Neuro-Impedance with Grey, Neuro-Impedance and Neural Controllers

V. Conclusion

In this paper, a neural network-based PID controller with impedance and grey prediction was applied to an artificial pneumatic muscle manipulator with unknown dynamics. The main motivation for this work was its applicability to planned future work of learning grasping affordances. The two submotions of a human arm were realized by combining artificial neural networks with the PID controller managed by impedance placed between an end-effector and a goal object. Grey predictors added to the PID controller improve the performance noticeably. The proposed PID controller with impedance was shown to be applicable to control the end-effector position for dexterous grasping and allowed ISAC to learn tool grasping by adaptively changing its virtual impedance parameters.

VI. Future Work

In the future, robots will be required to exhibit robust performance in a wide range of situations and accomplish increasingly complex tasks. Robotic control systems must evolve to handle such complex tasks. One promising approach is to advance the control technology beyond existing engineering-oriented approach to empower robots with human-like cognitive control capabilities [26]. For example, affect is one of the most important control features to accomplish conflicting goals across a broad range of dynamically changing circumstances in which robots are situated. Another important feature is for robots to learn affordances [27]. Affordance relations are an emergent property of the goal-situation relationship. By empowering robots how to learn affordances, robots will learn, from experience. Affordance learning has been recently studied for robot manipulators [28][29] and mobile robots [30]. We are modeling affordances as statistical relations between actual actions, object properties and the results or experiences of actions on objects and evaluating how the robot uses these affordances to execute the new tasks successfully.

Although ISAC has successfully demonstrated to be useful in human-robot coexisting environments in a lab setting [31][32], its arm movements were rather primitive and acting as a separate agent from our cognitive structure. In order to achieve more natural arm movements and better adaptability within our cognitive control architecture, we have developed the more distributed human-like controller. Our approach uses a hybrid artificial neural network- and vision-based impedance controller. This controller regulates the virtual impedance between ISAC arm and the external objects using the visual information. Unlike the conventional impedance controller, it uses the virtual interaction force to express the relationship between the manipulator and the environment without physical contact, so that the dynamics of the relative motion of ISAC arm to the object can be controlled using virtual force fields (i.e., non-contact impedance surfaces).

ACKNOWLEDGMENT

The authors extend their thanks to colleagues and Flo Wahidi in the Center for Intelligence Systems at Vanderbilt University for their assistance. This work is supported in part under NSF grant EIA0325641, "ITR: A Biologically Inspired Adaptive Working Memory System for Efficient Robot Control and Learning".

REFERENCES

[1] Y. Takeda, Y. Tanaka, T. Tsuji, "A virtual training sports system for measuring human hand impedance," *Proceedings of IEEE/ASME International Conference on Advanced Intelligent Mechatronics*, vol. 2, pp. 914-919, 2003.

[2] F. A. Mussa-Ivaldi, N. Hogan, and E. Bizzi, "Neural, Mechanical and Geometric Factors Subserving Arm in Humans," *Journal of Neuroscience*, vol. 5, No. 10, pp. 2733-2743, 1985.

[3] H. Gomi and M. Kawato, "Human m Stiffness and Equilibrium-point Trajectory during Multi-joint Movement," *Biological Cybernetics*, vol. 76, pp. 163-171, 1997.

[4] T. Tsuji, P. G. Morasso, K. Goto, K. Ito, "Human Hand Impedance Characteristics during Maintained Posture," *Biological Cybernetics*, vol. 72, pp. 457-485, 1995.

[5] C. P. Chou and B. Hannaford, "Static and dynamic characteristics of McKibben pneumatic artificial muscles," , *Proc. 1994 IEEE Robotics and Automation Conf.*, pp. 281-286, 1994.

[6] D. G. Caldwell, G. A. Medrano-Cerda, and M. Goodwin, "Control of pneumatic muscle actuators," *IEEE Control Syst. Mag.*, vol. 15, no. 1, pp. 40-48, 1995.

[7] J. H. Lilly and L. Yang, "Sliding mode tracking for pneumatic muscle actuators in opposing pair configuration," *IEEE Transactions on Control Systems Technology*, vol. 13, pp. 550-558, 2005.

[8] C. Chou and B. Hannaford, "Static and dynamic characteristics of mckibben pneumatic artificial muscles," *IEEE International Conference on Robotics and Automation* , vol. 1, pp. 281-286, 1994.

[9] M. Ozkan, K. Inoue, K. Negishia, and T. Yamanaka, "Defining a neural network controller structure for an artificial pneumatic muscle robot," *Neural Networks.*, vol. 13, pp. 533-544, 2000.

[10] J. Schroder, D. Erol, K. Kawamura, and R. Dillman, "Dynamic pneumatic actuator model for a model-based torque controller," *IEEE International Symposium on Computational Intelligence in Robotics and Automation.*, vol. 1, pp. 342-347, 2003.

[11] N. Tsagarakis, D. G. Caldwell, and G. A. Medrano-Cerda, "A 7 DOF pneumatic muscle actuator (pMA) powered exoskeleton," *IEEE International Workshop on Robot and Human Interaction*, pp. 327-333, 1999.

[12] K. Balasubramanian and K. S. Rattan, "Fuzzy logic control of a pneumatic muscle system using a linearing control scheme," *Fuzzy Information Processing Society*, pp. 432-436, 2003.

[13] T. Hesselroth, K. Sarkar, P. P. V. der Smagt, and K. Schulten, "Neural network control of a pneumatic robot arm," *IEEE Transactions on Systems, Man and Cybernetics*, vol. 24, no. 1, pp. 28-38, 1994.

[14] C. Lin and C. Lee, *Neural fuzzy systems : a neurofuzzy synergism to intelligent systems*, Prentice Hall, NJ, 1st edition, 1996.

[15] N. Hogan, "Impedance Control: An Approach to Manipulation, Parts 1,2,3," *ASME journal of Dynamic Systems, Measurement, and Control*, vol. 107, 1, pp. 1-24, 1985.

[16] E. Colgate and N. Hogan, "An Analysis of Contact Instability in terms of Passive Physical Equivalents," *Proc. of IEEE International Conference on Robotics and Automation*, pp. 404-409, 1989.

[17] Z. W. Luo and M. Ito, "Control Design of Robot for Compliant Manipulation on Dynamic Environments," *IEEE Trans. on Robotics and Automation,* Vol.9, No.3, pp. 286-296, 1993.

[18] N. Hogan, "Stable Execution of Contact Tasks Using Impedance Control," *Proc. of IEEE Intern. Conference on Robotics and Automation*, pp. 1047-1054, 1987.

[19] A. Castano and S. Hutchinson, "Visual Compliance:Task-Directed Visual Servo Control," *IEEE Trans. on Robotics and Automation*, vol. 9, no. 3, pp. 334-342, 1994.

[20] T. Tsuji, H. Akamatsu and M. Kaneko, "Non-Contact Impedance Control for Redundant Manipulators Using Visual Information," *Proc. of IEEE Intern. Conference on Robotics and Automation*, vol. 29, pp. 2571-2576, 1997.

[21] J. L. Deng, "Introduction to Grey System Theory," *The Journal of Grey System*, vol. 1, pp. 1-24, 1989.

[22] *Rubber actuator and air servo valve unit operation manual*, Bridgestone Robot Systems, Bridgestone Corporation, Tokyo, Japan, 1991.
[28] Rubbertuators and applications for robotics, Technical Guide 1, Bridgestone Corporation, Japan, 1986.

[23] E. Kayacan, O. Kaynak, "Grey Prediction Based Control of a Non-Linear Liquid Level System Using PID Type Fuzzy Controller," *IEEE International Conference on Mechatronics*, pp. 292-296, 2006.

[24] Y. Oniz, E. Kayacan, O. Kaynak, "Simulated and experimental study of antilock braking system using grey sliding mode control," IEEE International Conference on Systems, Man and Cybernetics, pp. 90-95, 2007.

[25] J. J. Craig, *Introduction to Robotics*, Addison-Wesley, 1998.

[26] K. Kawamura, S. Gordon, P. Ratanaswasd, E. Erdemir, J. Hall, "Implementation of Cognitive Control for a Humanoid Robot," submitted to *International Journal of Humanoid Robotics*, March 2008, Under Review.

[27] J. J. Gibson, *The Ecological Approach to Visual Perception*, Boston, MA, Houghton Mifflin, 1979.

[28] P. Fitzpatrick, G. Metta, L. Natale, S. Rao, G. Sandini, "Learning about objects through action - initial steps towards artificial cognition," *Proceedings of IEEE International Conference on Robotics and Automation(ICRA '03)*, vol. 3, pp. 3140-3145, 2003.

[29] A. Stoytchev, "Toward learning the binding affordances of objects: A behavior-grounded approach," *Proceedings of AAAI Symposium on Developmental Robotics*, pp. 21-23, 2005.

[30] E. Ugur, M. R. Dogar, M. Cakmak, E. Sahin, "The learning and use of traversability affordance using range images on a mobile robot," *IEEE International Conference on Robotics and Automation*, pp. 1721-1726, 2007.

[31] K. Kawamura, "Synthetic Approach to Cognitive Systems: A perspective from cognitive robotics," *IEEE/RSJ 2007 International Conference on Intelligent Robots and Systems (IROS)*, San Diego, CA, November 2, 2007.

[32] K. Kawamura, S. Gordon, P. Ratanaswasd, C. Garber, and E. Erdemir, "Implementation of Cognitive Control for Robots," *Proceedings of the 4th COE Workshop on Human Adaptive Mechatronics (HAM)*, 2007.